

# The NH---FC Dipole Orientation Effect for Pendant Exocyclic CH<sub>2</sub>F

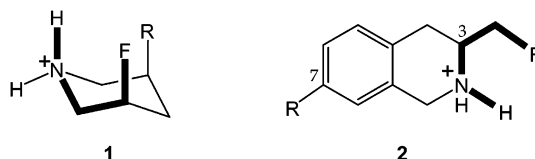
David C. Lankin,<sup>\*,†</sup> Gary L. Grunewald,<sup>‡</sup> F. Anthony Romero,<sup>‡</sup> Ilkay Yildiz Oren,<sup>§</sup> and James P. Snyder<sup>\*,§</sup>

Pharmacia Corporation, 4901 Searle Parkway/P-024, Skokie, Illinois 60077,  
Department of Medicinal Chemistry, University of Kansas, Lawrence, Kansas 66045,  
and Department of Chemistry, Emory University, Atlanta, Georgia 30322

snyder@euch4e.chem.emory.edu

Received June 12, 2002

## ABSTRACT



DFT and MMFF force field calculations for **2** (R = H) predict that two conformers dominate in water ( $\geq 95\%$ ) and both sustain a geometry in which the C–F and H–N dipoles align oppositely in a near-planar arrangement. The <sup>1</sup>H NMR spectra (D<sub>2</sub>O and DMSO-*d*<sub>6</sub>) and X-ray structure for **2** (R = SO<sub>2</sub>NHEt) confirm the predictions in all essentials. A novel single-conformer system is proposed.

It has been argued experimentally and theoretically that CF- -HN hydrogen bonds are both weak and infrequent.<sup>1–4</sup> While this observation may prove to be accurate as a broad generalization, a topological variant represents a powerful force at least as influential as a hydrogen bond; namely, the electrostatic association between appropriately oriented <sup>+</sup>N–H and C–F dipoles. The 3-fluoropiperidine structure **1** (R = H, CO<sub>2</sub><sup>-</sup>, F) is the prototype, preferring axial to equatorial fluorine by 96–100:1 in aqueous solution.<sup>5,6</sup>

For example, for **1** (R = F), the <sup>+</sup>N–H and C–F moieties are essentially coplanar ( $\phi(\text{N–H} \cdots \text{C–F}) = \pm 9^\circ$ ), while the geometry around them falls outside the normal ranges regarded as characterizing an H-bond ( $r(\text{F} \cdots \text{H}) = 2.40 \text{ \AA}$ ) and  $\theta(\text{N–H} \cdots \text{F}) = 102^\circ$ ).<sup>6</sup> Along with solvation effects,

the parallel but oppositely oriented <sup>+</sup>N–H and C–F bonds are sufficiently strong to overcome the halogen repulsion occasioned by a fluorine–fluorine separation of 2.81 Å (Becke3LYP/6-311G\* optimized<sup>6</sup>), 0.13 Å shorter than the sum of the Bondi van der Waals radii.<sup>7</sup>

In view of the relative rigidity of **1**, we sought an alternative structural framework with greater mobility to explore the generality of the conformer-directing NH/FC interaction. The 1,2,3,4-tetrahydroisoquinoline (THIQ) nucleus with a fluoromethyl group at C-3, **2**, was attractive for several reasons. First, the compound is flexible both within the saturated ring and at the easily rotated exocyclic C<sup>3</sup>–C(H<sub>2</sub>F) bond. Second, three of the six possible conformations (see below) potentially sustain the ideal planar NH/FC geometry across the five-atom fragment highlighted in bold in **1** and **2**. Third, the structure is of biological interest as it is a member of a family of potent and selective phenylethanolamine *N*-methyltransferase (PNMT) inhibitors, and the activity appears to owe its origin partly to the presence of the CH<sub>2</sub>F moiety.<sup>8</sup> In the present work, we examine the operation of the dipole–dipole effect in the novel analogue **2** (R = SO<sub>2</sub>–NH<sub>2</sub>)<sup>8d</sup> by application of density functional theory (DFT), molecular mechanics (MMFF), dynamic NMR, and X-ray spectroscopy.

(7) Bondi, A. J. *J. Phys. Chem.* **1964**, *68*, 441–451.

<sup>†</sup> Pharmacia Corp.

<sup>‡</sup> University of Kansas.

<sup>§</sup> Emory University.

(1) Murray-Rust, P.; Stallings, W. C.; Monti, C. T.; Preston, K. R.; Glusker, J. P. *J. Am. Chem. Soc.* **1983**, *105*, 3206–3214. Shimoni, L.; Glusker, J. P. *Struct. Chem.* **1994**, *5*, 383–397.

(2) Howard, J. A. K.; Hoy, V. J.; O'Hagan, D.; Smith, G. T. *Tetrahedron* **1996**, *38*, 12613–12632.

(3) Dunitz, J. D.; Taylor, R. *Chem. Eur. J.* **1997**, *3*, 89–98.

(4) Plenio, H.; Diodone, R. *Chem. Ber./Recl.* **1997**, *130*, 633–640.

(5) Lankin, D. C.; Chandrakumar, N. S.; Rao, S. N.; Spangler, D. P.; Snyder, J. P. *J. Am. Chem. Soc.* **1993**, *115*, 3356–3357.

(6) Snyder, J. P.; Chandrakumar, N. S.; Sato, H.; Lankin, D. C. *J. Am. Chem. Soc.* **2000**, *122*, 544–545.

Prior to our empirical structural studies, density functional theory at the Becke3LYP/6-311G(d,p) level<sup>9,10</sup> was used to optimize the six conformations of **2**. These arise from the two twist-chair conformations of the unsaturated tetrahydropyridine ring, each of which sustains three conformers by rotation about the exocyclic C–C(F) bond. The results are listed in Table 1, while the structures of the three lowest

**Table 1.** Relative Energies and Selected Geometric Variables for Conformers of **2** (R = H) Optimized with DFT (Becke3LYP/6-311G(d,p)) and the MMFF Force Field; MP2/6-311G(d,p) Single-Point Energies

	$\Delta E(\text{rel})$ (kcal/mol)			dist <sup>a</sup> (Å)		
	Becke3LYP <sup>c</sup>	MP2 <sup>c</sup>	MMFF <sup>d</sup>	F–H	$\phi^b$ (deg)	
	gas	H <sub>2</sub> O <sup>e</sup> (%)	H <sub>2</sub> O <sup>e</sup> (%)	H <sub>2</sub> O <sup>e</sup> (%)		
<b>2a</b>	0.0	0.0 (79)	0.0 (69)	0.0 (84)	2.18	–3.5
<b>2b</b>	0.8	1.0 (15)	0.9 (15)	1.2 (11)	2.35	–9.5
<b>2c</b>	1.2	1.6 (5)	0.9 (15)	1.7 (5)	2.22	11.2
<b>2d</b>	4.6	2.8 (0.7)	2.8 (0.6)	3.0 (0.5)	<i>f</i>	
<b>2e</b>	5.9	3.7 (0.2)	3.5 (0.2)	4.4 (0.1)	<i>f</i>	
<b>2f</b>	6.8	4.6 (0.0)	3.9 (0.1)	5.1 (0.0)	<i>f</i>	

<sup>a</sup> DFT CF–H separation. <sup>b</sup> DFT improper torsion. <sup>c</sup> DFT optimized and MP2 single point, 6-311G\*\* basis set, PCM/H<sub>2</sub>O model. <sup>d</sup> MMFF, GBSA/H<sub>2</sub>O model. <sup>e</sup> Boltzmann distribution at 25 °C. <sup>f</sup> Distance > 3.2 Å.

energy forms and the third equatorial conformer are depicted in Figure 1. As judged by DFT calculations, members of the low energy trio all sustain the near-planar C–F–H–N association with F–H separations of 2.2–2.4 Å (Table 1). The global minimum **2a** and the next lowest energy conformer **2b** both locate the CH<sub>2</sub>F group in a pseudoequatorial arrangement. However, the dipole-oriented C–F and N–H bonds are disposed equatorially and axially, respectively. Next in energy is a structure with an axial CH<sub>2</sub>F aligned with an equatorial NH bond, **2c**. In the PCM continuum water model, these three forms are predicted with populations of 79, 15, and 5% accounting for 99% of the

(8) (a) Grunewald, G. L.; Dahanukar, V. H.; Jalluri, R. K.; Criscione, K. R. *J. Med. Chem.* **1999**, *42*, 1982–1990. (b) Grunewald, G. L.; Caldwell, T. M.; Li, Q.; Criscione, K. R. *J. Med. Chem.* **1999**, *42*, 3588–3601. (c) Grunewald, G. L.; Caldwell, T. M.; Li, Q.; Criscione, K. R. *J. Med. Chem.* **2001**, *44*, 2849–2856. (d) Grunewald, G. L.; Romero, F. A.; Criscione, K. R. Submitted for publication.

(9) Frisch, M. J.; Trucks, G. W.; Schlegel, H. B.; Scuseria, G. E.; Robb, M. A.; Cheeseman, J. R.; Zakrzewski, V. G.; Montgomery, J. A., Jr.; Stratmann, R. E.; Burant, J. C.; Dapprich, S.; Millam, J. M.; Daniels, A. D.; Kudin, K. N.; Strain, M. C.; Farkas, O.; Tomasi, J.; Barone, V.; Cossi, M.; Cammi, R.; Mennucci, B.; Pomelli, C.; Adamo, C.; Clifford, S.; Ochterski, J.; Petersson, G. A.; Ayala, P. Y.; Cui, Q.; Morokuma, K.; Malick, D. K.; Rabuck, A. D.; Raghavachari, K.; Foresman, J. B.; Cioslowski, J.; Ortiz, J. V.; Stefanov, B. B.; Liu, G.; Liashenko, A.; Piskorz, P.; Komaromi, I.; Gomperts, R.; Martin, R. L.; Fox, D. J.; Keith, T.; Al-Laham, M. A.; Peng, C. Y.; Nanayakkara, A.; Gonzalez, C.; Challacombe, M.; Gill, P. M. W.; Johnson, B. G.; Chen, W.; Wong, M. W.; Andres, J. L.; Head-Gordon, M.; Replogle, E. S.; Pople, J. A. *Gaussian 98*, revision A.1; Gaussian, Inc.: Pittsburgh, PA, 1998.

(10) DFT theory has been successfully applied to a number of systems involving ammonium cations: Ha, Y. L.; Chakraborty, A. K. *J. Phys. Chem.* **1992**, *96*, 6410–6417. Wolken, J. K.; Turecek, F. *J. Am. Chem. Soc.* **1999**, *121*, 6010–6018. Howard, S. T.; Fallis, I. A. *J. Chem. Soc., Perkin Trans. 2* **1999**, 2501–2506. Kinbara, K.; Oishi, K.; Harada, Y.; Saigo, K. *Tetrahedron* **2000**, *56*, 6641–6655.

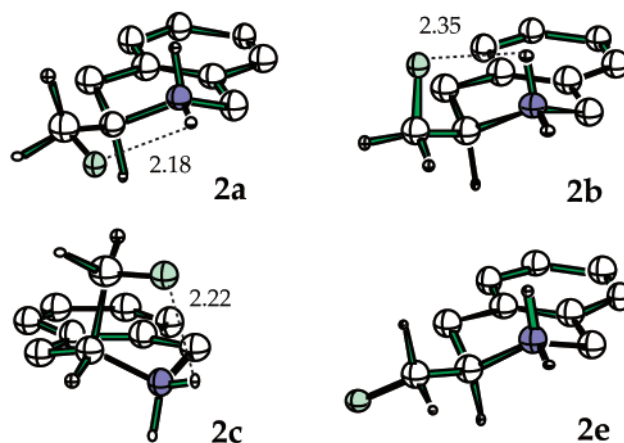


**Figure 1.** Optimized geometries for the lowest three Becke3LYP/6-311G(d,p) conformers **2a–c** showing the CF–H distances (Å). **2e** is the high energy CH<sub>2</sub>F pseudoequatorial form.

total. The remaining three conformers, one of which carries an equatorial CH<sub>2</sub>F with the C–F bond directed away from NH<sub>2</sub><sup>+</sup> (**2e**), are all posited to be 2.8–4.6 kcal/mol above the global minimum. Supplemental MP2/6-311G(d,p) single-point energies at the DFT geometries lead to the same outcome.

Very similar results were obtained with the MMFF(94) force field<sup>11–15</sup> in MacroModel<sup>16</sup> using the GBSA/H<sub>2</sub>O continuum water model<sup>17</sup> (Table 1). Conformers **2a** and **2b** are once again the two lowest energy forms with **2c** slightly higher. Thus, both in the DFT and the MMFF molecular mechanics frameworks, the stability order of the six conformers and the energy differences are nearly identical.

A series of 2-D NMR spectra for **2** (R = SO<sub>2</sub>NH<sub>2</sub>) were measured in both D<sub>2</sub>O and DMSO-*d*<sub>6</sub> solvents at 500 MHz. All carbons and hydrogens were assigned. Chemical shifts and *J*<sub>HH</sub> and *J*<sub>HF</sub> couplings are virtually identical in the two solvents (see the Supporting Information). We take two approaches to deconvoluting the averaged NMR spectra to estimate populations of the various conformers in solution. The first relies on <sup>3</sup>*J*<sub>H3–F</sub> with values of 21.9 and 20.2 Hz in DMSO-*d*<sub>6</sub> and D<sub>2</sub>O, respectively and makes the assumption that **2a** and **2b** are the sole conformations observable. The DFT-optimized geometries report the F–C–C3–H dihedral angles as 62.7 and 167.9°, respectively. Application of

(11) The MMFF force field has not only been parametrized for C–F bonds and piperidines (ref 13), but the approach yields quite reasonable conformational energy differences for molecules containing these functional groups (ref 15). The polar interactions between the N–H and C–F bonds are handled by buffered Coulombic ESP charges at the HF/6-31G\* level (ref 12).

(12) Halgren, T. A. *J. Comput. Chem.* **1996**, *17*, 490–519.

(13) Halgren, T. A. *J. Comput. Chem.* **1996**, *17*, 6165–641.

(14) Halgren, T. A.; Nachbar, R. B. *J. Comput. Chem.* **1996**, *17*, 587–615.

(15) Halgren, T. A. *J. Comput. Chem.* **1999**, *20*, 730–748.

(16) (a) Mohamadi, F.; Richards, N. G. J.; Guida, W. C.; Liskamp, R.; Lipton, M.; Caufield, C.; Chang, G.; Hendrickson, T.; Still, W. C. *J. Comput. Chem.* **1990**, *11*, 440–467. (b) Cf. www.schrodinger.com/macromodel2.html.

(17) Still, W. C.; Tempczyk, A.; Hawley, R. C.; Hendrickson, T. *J. Am. Chem. Soc.* **1990**, *112*, 6127.

Thibaudeau and colleagues' seven-parameter Karplus equation for vicinal F/H coupling<sup>18</sup> translates the latter to individual couplings of  ${}^3J_{\text{H3-F}}(\mathbf{2a}) = 11.9$  and  ${}^3J_{\text{H3-F}}(\mathbf{2b}) = 47.5$  Hz, respectively. Under the conditions that conformers **2a** and **2b** are rapidly averaged and the populations sum to 100% ( $(a + b) = 1$ ), the equation  $J_{\text{avg}} = aJ(\mathbf{2a}) + bJ(\mathbf{2b})$  can be solved for the populations. Thus, we obtain  $[\mathbf{2a}]/[\mathbf{2b}] = 72:28$  and  $77:23$  in DMSO-*d*<sub>6</sub> and D<sub>2</sub>O, respectively.<sup>19</sup>

The second approach utilizes four three-bond proton–proton coupling constants from H3 to define the spatial orientation of the CH<sub>2</sub>(F) protons:  ${}^3J_{\text{H3-CH2F(A)}} = 5.3$  Hz,  ${}^3J_{\text{H3-CH2F(B)}} = 2.9$  Hz,  ${}^3J_{\text{H3-H4A}} = 11.1$  Hz, and  ${}^3J_{\text{H3-H4B}} = 5.1$  Hz (DMSO-*d*<sub>6</sub>). For this analysis, we employ the NAMFIS procedure,<sup>20</sup> which has proven useful for deconvoluting the average NMR spectra of complex antitumor natural products into individual conformations with estimated populations.<sup>21,22</sup> All six DFT-optimized conformations (Table 1) served as the database of candidate structures. The best fit of the coupling constants gives a very low sum of square differences ( $SD = 0.20$ )<sup>23</sup> and three contributing conformations: **2a** (56%), **2b** (33%), and **2f** (10%). The latter high energy conformer (4.6–6.8 kcal/mol above the global minimum) is clearly an artifact. Following removal of the three high energy conformers **2d–f** (Table 1) from the dataset, NAMFIS returns only **2a** and **2b** as solutions to the  ${}^3J_{\text{H-H}}$  average (populations of 58 and 42%, respectively), rejecting **2c** as incompatible with the measured coupling constants. Although both quantum and molecular mechanics posit an observable population of **2c** (Table 1), when **2** is dissolved in solution with explicit hydrogen bonding between substrate and solvent, the population of this conformer would appear to fall below that estimated by the continuum models. As to **2a** and **2b**, the populations obtained are in complete accord with the values derived from  ${}^3J_{\text{H-F}}$ .

On the basis of the analysis of both proton–fluorine and proton–proton coupling constants, it appears that salt **2** in solution exists as a rapidly exchanged mixture of **2a** and **2b** in which the former dominates by approximately 1.4–2.3:1 (i.e., 60:40 ± 10%). Support for the global stability of **2a** as predicted by DFT and derived by NMR is the X-ray crystal structure of **2** ( $R = \text{SO}_2\text{NHEt}$ ) depicted in Figure 2. The latter structure is the conformation shown in Figure 1, **2a**. Key parameters are  $r(\text{F} \cdots \text{H}) = 2.49$  Å and  $\phi(\text{FC} \cdots \text{HN}) = -11.3^\circ$  (cf. Table 1).

Considering the ability of the DFT and MMFF calculations to accurately represent the two dominant conformers of **2**, we have made predictions for four simple analogues as depicted in Scheme 1. In each case, we probed the relative

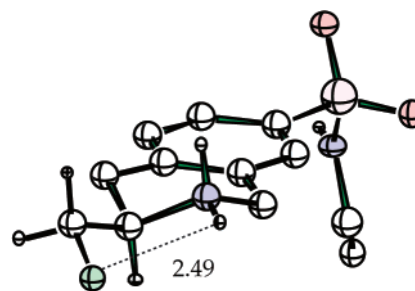
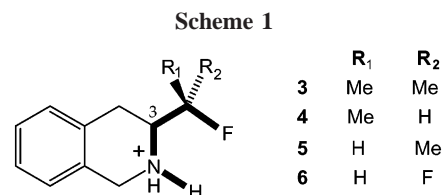


**Figure 2.** X-ray structure of 3-fluoromethyl-7-*N*-(ethylamino-sulfonyl)-1,2,3,4-THIQ·HCl; CF...NH distance in Å.

stability of the analogues of **2a/b** by MMFF optimization and subsequent graphical verification that the structures adopt the same conformational minima. Modifications of **3** ( $R_1 = R_2 = \text{Me}$ ) and **4** ( $R_1 = \text{H}$ ,  $R_2 = \text{Me}$ , *pro-S*) suggest that the **a** and **b** conformers sustain about the same 60:40 ratio as **2**.



On the other hand, the *pro-R* structure **5** ( $R_1 = \text{Me}$ ,  $R_2 = \text{H}$ ) is predicted to invert the ratio so that  $[\mathbf{a}]/[\mathbf{b}] = 55:45$ . The most immobile system is **6**, in which two fluorines reside on the exocyclic carbon. In this case, both C–F bonds are partnered with an N–H bond in the **a**-form, one equatorial, the other axial (Figure 3). MMFF/GBSA/H<sub>2</sub>O posits that the

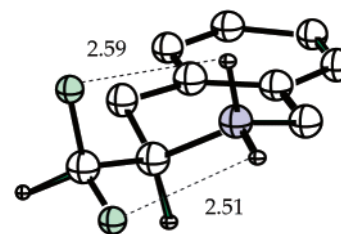


**Figure 3.** CHF<sub>2</sub>-containing structure **6** predicted to exist in a single conformation; MMFF/GBSA/H<sub>2</sub>O optimized; CF...NH distances in Å.

system exists in this single conformation, all other forms falling 3–4 kcal/mol higher in energy.

Although the CF<sub>2</sub>H group is larger than CH<sub>3</sub>, steric effects cannot account for the conformational rigidity predicted for **6**. The latter sustains 1,5-F...H(N) MMFF distances of 2.51–2.59 Å and a 1,5-F...H(C) separation of 2.56 Å. Each

(18) Thibaudeau, C.; Plavec, J.; Chattopadhyaya, J. *J. Org. Chem.* **1998**, *63*, 4967–4984.

(19) The  $J(\text{H,F})$  Karplus parametrization of ref 12 is based on HF/3-21G-optimized geometries. For compatibility with that work, the populations quoted here were derived with similarly optimized structures.

(20) Cicero, D. O.; Barbato, G.; Bazzo, R. *J. Am. Chem. Soc.* **1995**, *117*, 1027–1033.

(21) Snyder, J. P.; Nevins, N.; Cicero, D. O.; Jansen, J. *J. Am. Chem. Soc.* **2000**, *122*, 724–725.

(22) Monteagudo, E.; Cicero, D. O.; Cornett, B.; Myles, D. C.; Snyder, J. P. *J. Am. Chem. Soc.* **2001**, *123*, 6929–6930.

(23) Nevins, N.; Cicero, D.; Snyder, J. P. *J. Org. Chem.* **1999**, *64*, 3979–3986.

of these is somewhat below the sum of H and F van der Waals distances, 2.67 Å.<sup>24</sup> By contrast, the higher energy conformers show similar F...H(N) distances but longer 1,5-F...H(C) gaps of 2.61–2.70 Å.

In conclusion, the CF/HN dipole–dipole interaction that powers the conformational equilibria of protonated fluoropiperidines to favor axial fluorine<sup>5,6</sup> carries over without exception to an analogue in which the C–F fluorine bond is exocyclic to the ring. In the present case, the multiple-conformer system **2** in either D<sub>2</sub>O or DMSO-*d*<sub>6</sub> favors two conformers, both of which enjoy electrostatic stabilization. The global minimum, predicted by the Becke3LYP/6-311G-(d,p) DFT recipe, operates not only in solution but also in the solid state. It can be anticipated that the CF/HN dipole–dipole phenomenon will prove to express itself in a wide array of biologically active compounds containing fluorine.<sup>25</sup> For example, the fluorinated piperidine subclass has recently been explored as serotonin-subtype receptor ligands,<sup>26–28</sup> α<sub>2</sub>-adrenoceptor ligands,<sup>8</sup> and phenylethanolamine *N*-methyltransferase (PNMT) inhibitors.<sup>8</sup> In the latter case, the 1,2,3,4-

tetrahydroisoquinoline (THIQ) nucleus furnishes highly selective inhibitors with the ability to penetrate the blood–brain barrier when substituted with a fluoromethyl group at C-3 and an electron-withdrawing moiety at C-7, i.e., **2**. It will be of interest to learn if the CF/HN dipole–dipole geometry persists in an X-ray structure of a PNMT–THIQ complex. As a complement to the CF/HN electrostatic effect, it has been reported recently that a series of hydroxylated piperidines evidence a consistent increase in nitrogen basicity when an OH β or γ to the amine is axial (Δp*K*<sub>a</sub> = 0.8).<sup>29</sup> Here, the OH moiety plays the role discussed above for F. In a related case, replacement of S<sup>+</sup> for N<sup>+</sup> and OH for F likewise leads to an unusual axial–axial arrangement for a castanospermine analogue.<sup>30</sup> We expect that the stereodirecting effect of fluorine in combination with ammonium cations, and perhaps sulfonium cations, will prove to have important consequences for drug binding, synthetic control, and the design of new materials.

**Acknowledgment.** The work was supported in part by the National Institutes of Health (HL34193), the American Foundation for Pharmaceutical Education, and the American Heart Association. We thank Dr. Douglas R. Powell (University of Kansas) for the crystal structure of **2**. DFT calculations were performed at the Cherry Emerson Center for Computational Chemistry, Emory University.

**Supporting Information Available:** Tables of <sup>1</sup>H and <sup>13</sup>C NMR data and the X-ray structure cif file for **2** (R = SO<sub>2</sub>NHEt). This material is available free of charge via the Internet at <http://pubs.acs.org>.

OL026358C

(29) Jensen, H. H.; Lyngbye, L.; Jensen, A.; Bols, M. *Chem. Eur. J.* **2002**, *8*, 1218–1226.

(30) Svansson, L.; Johnston, B. D.; Gu, J.-H.; Patrick, G.; Pinto, B. M. *J. Am. Chem. Soc.* **2000**, *122*, 10769–10775.

(24) Bondi, A. *J. Phys. Chem.* **1964**, *68*, 441–451.

(25) (a) *Biomedical Aspects of Fluorine Chemistry*; Filler, R.; Kobayashi, Y., Ed.; Elsevier Science Pub. Co.: New York, 1982. (b) *Biomedical Frontiers of Fluorine Chemistry*; Ojima, I.; McCarthy, J. R.; Welch, J. T., Eds.; ACS Symposium Series No. 639; American Chemical Society: Washington, DC, 1996. (c) O'Hagan, D.; Rzepa, H. S. *Chem. Commun.* **1997**, 645–652. (d) Park, B. K.; Kitteringham, N. R.; O'Neill, P. M. Metabolism of fluorine-containing drugs. *Annu. Rev. Pharmacol. Toxicol.* **2001**, *41*, 443–470.

(26) van Niel, M. B.; Collins, I.; Beer, M. S.; Broughton, H. B.; Cheng, S. K. F.; Goodacre, S. C.; Heald, A.; Locker, K. L.; MacLeod, A. M.; Morrison, D.; Moyes, C. R.; O'Connor, D.; Pike, A.; Rowley, M.; Russell, M. G. N.; Sohal, B.; Stanton, J. A.; Thomas, S.; Verrier, H.; Watt, A. P.; Castro, J. L. *J. Med. Chem.* **1999**, *42*, 2087–2104.

(27) Hallett, D. J.; Gerhard, U.; Goodacre, S. C.; Hitzel, L.; Sparey, T. J.; Thomas, S.; Rowley, M. *J. Org. Chem.* **2000**, *65*, 4984–4993.

(28) Rowley, M.; Hallett, D. J.; Goodacre, S.; Moyes, C.; Crowthorpe, J.; Sparey, T. J.; Patel, S.; Marwood, R.; Patel, S.; Thomas, S.; Hitzel, L.; O'Connor, D.; Szeto, N.; Castro, J. L.; Hutson, P. H.; MacLeod, A. M. *J. Med. Chem.* **2001**, *44*, 1603–1614.